Design of a Low Power Hybrid Electro-Optic Plasmonic Modulator Based on ITO and Graphene

Omid Abbaszadeh-Azar
Shahid Beheshti University
Kambiz Abedi (k_abedi@sbu.ac.ir)
Shahid Beheshti University https://orcid.org/0000-0001-5014-1037

Research Article

Keywords: Graphene, ITO, Hybrid plasmonic, Silicon on insulator, Modulator

Posted Date: June 14th, 2021

DOI: https://doi.org/10.21203/rs.3.rs-578226/v1

Design of a Low Power Hybrid Electro-optic Plasmonic Modulator Based on ITO and Graphene

Omid Abbaszadeh-Azar, Kambiz Abedi*

Faculty of Electrical Engineering, Shahid Beheshti University,Tehran, Iran

**email: k_abedi@sbu.ac.ir*

Abstract:

In this paper, a hybrid plasmonic modulator based on ITO and graphene has been proposed and designed. Graphene and ITO are used in the active region, which increases the light-matter interaction and reduces the device's operating voltage in the proposed modulator. As a result, it increases the extinction ratio (ER), reduces power consumption and device footprint in the proposed modulator compared to similar modulators. The values of 14 dB/μm and 5.4 fJ are obtained for ER and power consumption, respectively. The time-domain finite-difference (FDTD) method is used to simulate the modulator. The integration of a modulator with high light-matter interaction and low power consumption in the silicon-on-insulator platform has significant potential for broadband, compact and efficient communication interconnects and circuits.

Keywords: Graphene, ITO, Hybrid plasmonic, Silicon on insulator, Modulator

1. Introduction

One of the key elements in optical electronics is the silicon-based optical modulator, connecting the two fields of photonics and electronics by converting an electrical signal into an optical signal. The key characteristics of the optical modulator are low power consumption, compact size, high extinction ratio (ER), and low insertion losses. Therefore, designing optical modulators with optimum parameters is essential. The architecture of typical modulators such as silicon-based structures [1, 2], high-quality resonant structures [3, 4], and Mach Zehnder structures [5, 6] are rarely able to optimize all modulator parameters simultaneously. Such structures have drawbacks such as narrow bandwidth, high-energy consumption as well as large size. Development of new modulators with compact size and broadband is required [7]. Metal oxide semiconductor-based hybrid plasmonic waveguides are used to design compact, broadband silicon-based optical modulators. These waveguides use doped silicon, Indium Tin Oxide (ITO), vanadium dioxide, or graphene [7-11]. A fundamental characteristic of these materials is adjusting the density of carriers and injecting charge into the material by applying an electric field [12-16]. Recently, directional coupler-based devices have been investigated [8, 9, 17]. In these structures, by changing the density of plasmonic material carriers in the coupler, the coupling rate and attenuation coefficient change, and the input signal can be modulated.

Plasmonic structures enhance light-matter interaction in optical devices and forming a strong local field interaction with plasmonic resonances. Based on this, combined plasmonic waveguide modulators (HPW) [12, 16, 18-20] and Metal-Insulator-Metal (MIM) [21, 22] have been introduced. In these structures, high confinement of the optical field leads to increasing interaction of light and matter. In recent years, the use of graphene as an active element in optical modulators has been considered. Graphene has unique properties such as a unique linear energy band, high carrier mobility at room temperature, and controllable light transmission and carrier density by applying electric media. These properties have led to the widespread use of graphene in electro-optical modulators from the visible range to terahertz [23-28]. However, these structures suffer from low ER due to poor interaction between graphene and light-wave. Therefore,

increasing the interaction between optical signals with graphene is very important to achieve optical devices that use graphene adjustability [29].

On the other hand, ITO-based modulators have high ER but suffer from high operating voltages and high power consumption. The ITO layer can be used in graphene plasmonic waveguides to increase graphene-based modulator and optical signal interaction [29, 30].

In this paper, a plasmonic modulator based on ITO and graphene is proposed and designed. The modulator structure consists of two silicon waveguides which a coupler is coupling these two waveguides. The coupler consists of Si/Graphene/HfO_2/ITO/HfO_2/Graphene vertical stack. The use of ENZ properties of both graphene and ITO materials has led to the design of modulators with low operating voltage and high resolution. The optical properties of the proposed modulator are investigated using the FDTD method.

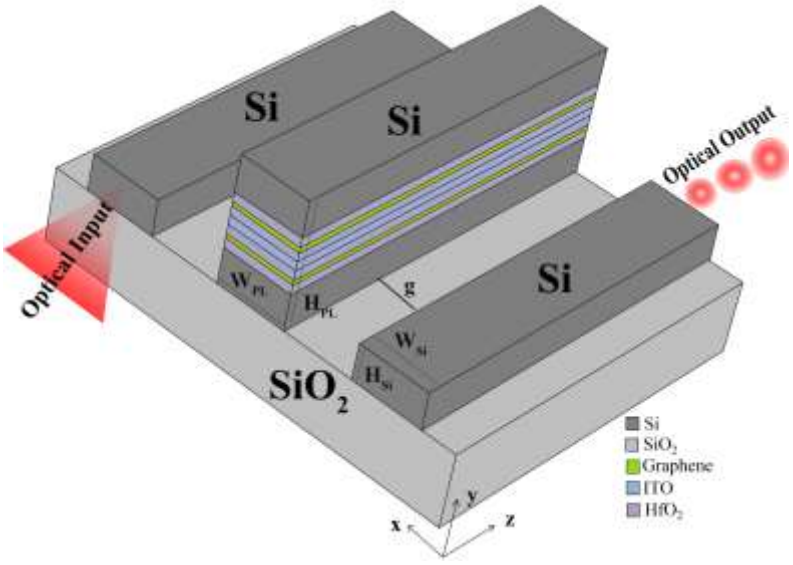

Figure 1: 3D view of the proposed structure

2. Configuration and Characterization of hybrid plasmonic waveguide

Figure 1 shows the proposed modulator structure, which consists of three waveguides. Two of them are silicon waveguides, and one is a plasmonic waveguide, which the plasmonic waveguide placed between the two silicon waveguides. The plasmonic waveguide is composed of ITO and multilayer graphene separated by HfO_2 dielectric and two silicon layers. The ITO and graphene layers are sandwiched between two layers of silicon.

The height and width of the two outer silicone waveguides H_{Si} and W_{Si} are assumed. The width and height of the middle waveguide are W_{PL} and H_{PL}, respectively. The height of the ITO layer is H_{ITO}, and the height of the HfO_2 layer is H_{HfO2}.

To investigate the epsilon near zero (ENZ) effect of two materials (ITO and graphene), we model the ITO and graphene using the Drude-Lorentz model and the Kubo formula, respectively.

At first, the refractive index of graphene will be investigated, which is related to its dynamic conductivity. The conductivity of graphene can be described using the Kobo equation, which includes intraband and the interband ($\sigma = \sigma_{intra} + \sigma_{inter}$), as follows [23, 31, 32]:

$$\sigma(\omega)=\frac{-ie^2}{\pi\mathrm{h}^2(\omega+i2\Gamma)}\left(\frac{\mu_c}{k_BT}+2\left(e^{\frac{-\mu_c}{k_BT}}+1\right)\right)+\frac{-ie^2(\omega+i2\Gamma)}{\pi\mathrm{h}^2}\left[\int_0^{\infty}\frac{\partial f_d(-\varepsilon)-\partial f_d(\varepsilon)}{(\omega+i2\Gamma)^2-4\left(\varepsilon/\mathrm{h}\right)^2}d\varepsilon\right] \quad (1)$$

Where k_B is the Boltzmann constant, T is the temperature, $f_d(\varepsilon)=\left(e^{\varepsilon-\mu_c/k_BT}+1\right)^{-1}$ is the Fermi–Dirac distribution, h is the reduced Planck's constant, μ_c is the chemical potential, $\Gamma=1/\tau$ is the charged particle scattering rate, and ω is the angular frequency.

The relationship between voltage and chemical potential is defined $\mu_c=\mathrm{h}v_F\sqrt{\pi|a_0V|}$, where v_F is the Fermi velocity in graphene and $a_0=9\times10^{16}m^{-2}V^{-1}$.

Surface permittivity is obtained using graphene conductivity ($\sigma=\sigma_{\mathrm{int}ra}+\sigma_{\mathrm{int}er}=\sigma'+i\sigma''$), at room temperature and λ = 1.55 μm:

$$\varepsilon_g=1+\frac{i\sigma(\omega,\mu_c)}{\omega\varepsilon_0\delta} \quad (2)$$

$\delta=1nm$ is the effective thickness of graphene [31, 32]. The real part of the permittivity changes from positive to negative values as the chemical potential increased [31].

An ITO layer has been used in the plasmonic waveguide to increase the interaction between the graphene and optical fields [33]. The ITO permittivity is described using the Drude-Lorentz model (equation 1) [34, 35].

$$\varepsilon=\varepsilon_\infty-\frac{\omega_p^2}{\omega^2+i\gamma\omega} \quad (3)$$

$$\omega_p^2=\frac{N\,e^2}{\varepsilon_\infty m^*} \quad (4)$$

$\varepsilon_\infty=3.9$ is the high-frequency permittivity of ITO. $m^*=0.35m_0$ is the effective mass of electrons, and e, m_0 indicates the charge and mass of electrons. ω_p is plasma frequency, and $\gamma=1.84\times10^{14}\,rad/s$ represents electron scattering rate. N is the carrier concentration of electrons in the ITOs accumulation layer, which its thickness is 1nm (W_a) according to the Tomas-Fermi screening theory [8, 36]. N is described as a function of voltage (V) as below equation [37]:

$$N=N_0+\frac{\varepsilon_0.\varepsilon_{HfO_2}.V}{e.H_{HfO_2}.W_a} \quad (5)$$

It was assumed that $N_0=1\times10^{19}\,\mathrm{cm}^{-3}$, $\varepsilon_{HfO_2}=25$, $H_{HfO_2}=10\mathrm{nm}$, $W_a=1\mathrm{nm}$ and ε_0 is the vacuum permittivity. High charge concentration in accumulation layers is reachable because of the high DC permittivity of HfO_2 ($\varepsilon_{HfO_2}=25$). As voltage increases, the carrier concentration in the accumulation layer and the imaginary part of permittivity increases. The real part of ITO's permittivity changes from positive to zero (ENZ state) and negative values, and as a result, the ITO changes from dielectric state to metallic state [38]. In the ENZ state, the electrical displacement components must be continuous at the interface of the ITO and dielectric ($\varepsilon_{HfO_2}E_{HfO_2}=\varepsilon_{ITO}E_{ITO}$). It causes significant confinement of the electrical field in the ITO and dielectric interface, and it improves the interaction of light and matter.

Figure 2(a) shows the propagation loss, and figure 2(b) shows the effective index of the device with two mono-graphene layers. The propagation loss has two peaks (one in 0.65 V and the other in 2.62 V) related to the ENZ effect in graphene and the other to the ENZ effect in the ITO. The first peak is affected by the chemical potential of graphene, and the second peak is related to the ITO. Because the impact of ENZ on graphene has occurred at a lower voltage, if the two peaks are combined by increasing the number of graphene layers, a lower operating voltage is achieved. Modulators with this effect could have higher efficiency and lower energy consumption [39].

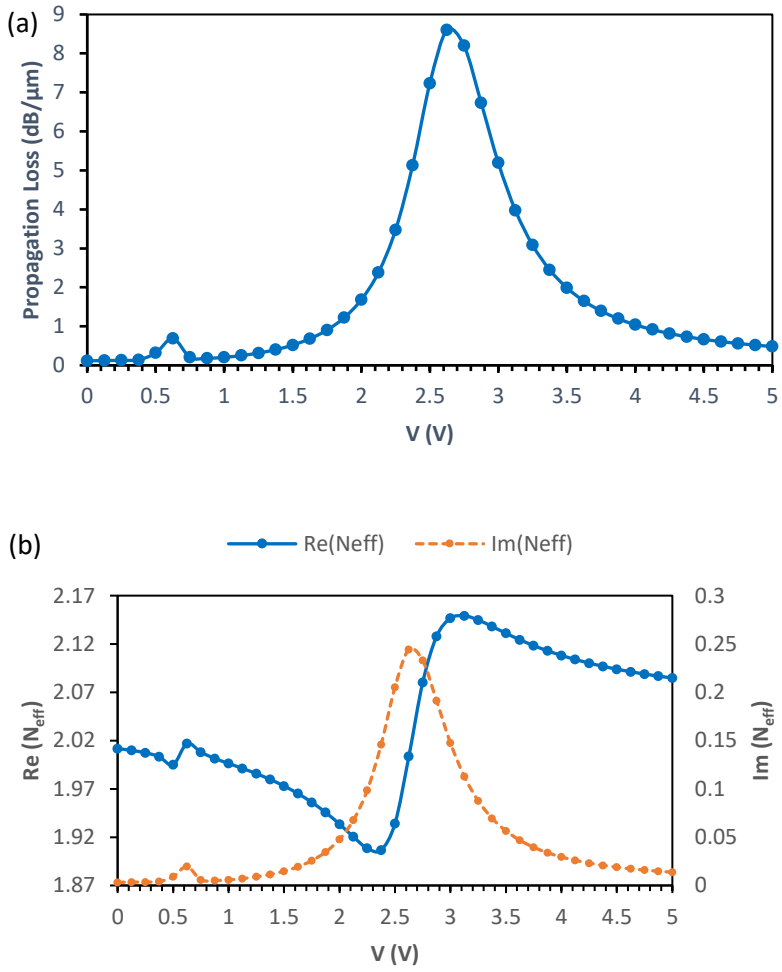

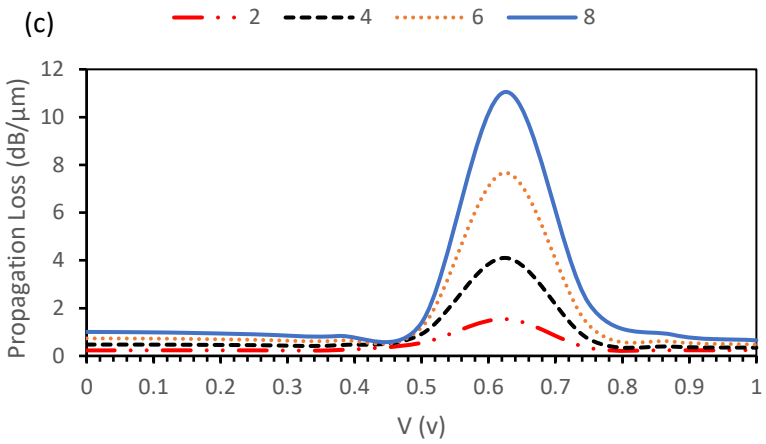

Figure 2: a) propagation loss for different voltage values (monolayer graphene) b) The real and imaginary part of the refractive index (graphene monolayer) c) propagation loss for different voltage values (multilayer graphene: 2,4,6,8 layer) (W_{PL}=130nm, H_{ITO}=10nm, H_{HfO2}=10nm)

As the number of graphene layers increases, the two peaks propagation loss due to the effect of ENZ on graphene and ITO merged, and the propagation loss at voltage 0.62 V increases (figure 2 (c)). Also, The use of a large number of graphene layers will cause the properties of graphite, and the effect of ENZ will be attenuation. Therefore, we consider 8 layers of graphene.

The intensity of the guided mode in on state (0 V) and in the off state (0.62 V) is shown in figure 3(b) and 3(c), respectively. The intensity of the guided mode in 0 V is distributed in the active layers in the coupling region (Figure 3(b)). In the 0.62 V, it is concentrated in the ITO and graphene layer (Figure 3(c)), and high losses occur due to the ENZ effect.

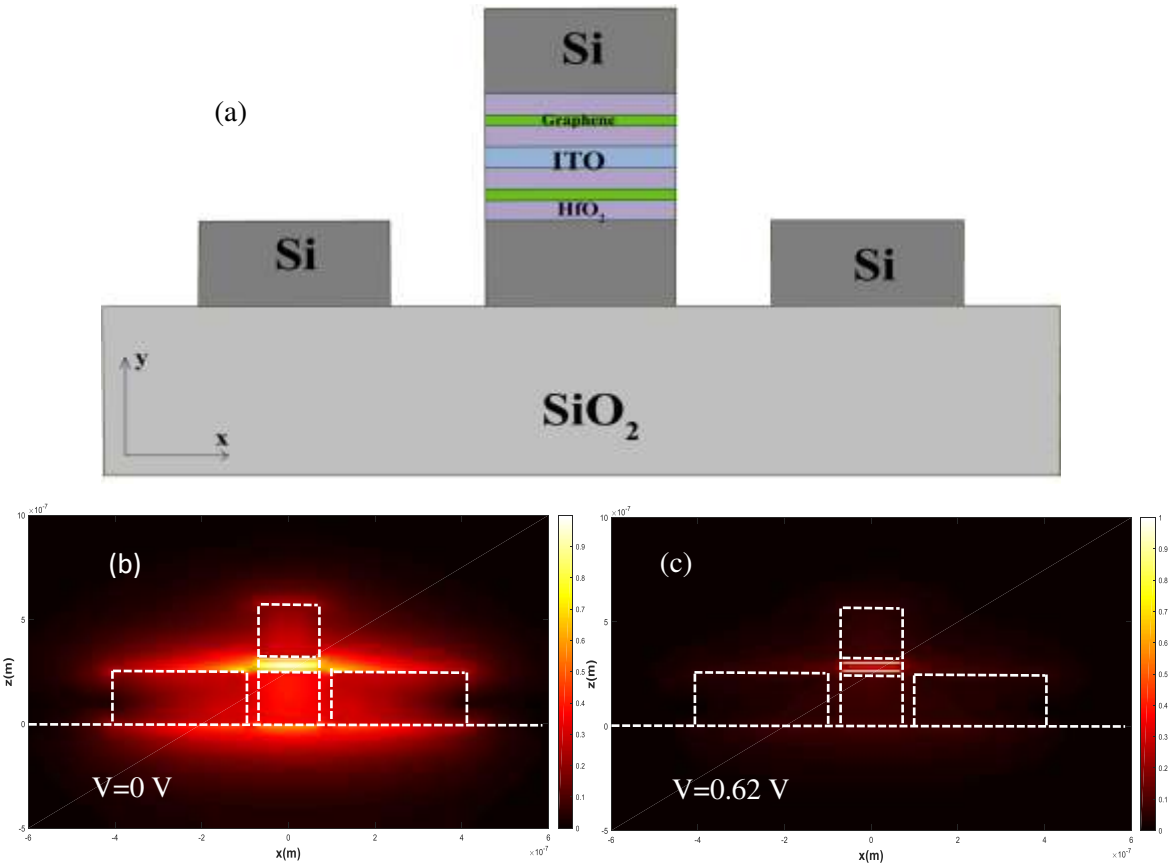

Figure 3: a) Proposed modulators cross-section view, the intensity of the guided mode of the electric field in b) On state (V=0) c) Off state (V=0.62V) (W_{Si}=300nm, H_{Si}=250nm, H_{PL}=566 nm ,W_{PL}=130nm, H_{ITO}=10nm, H_{HfO2}=10nm, g=30 nm)

3. Design and Simulation of modulator

The device was simulated with the FDTD method in 1.55 µm wavelength. The refractive index of the materials is assumed to be: $n_{si} = 3.47$, $n_{SiO_2} = 1.44$ and $n_{HfO_2} = 1.98$ [40]. W_{Si}=300nm and H_{Si}=250 nm are assumed to have a device with a compact size. For smaller sizes (W_{Si}<300 nm), the guided mode did not support.

The effective index of silicon and plasmonic waveguides should be matched to increase the coupling rate between waveguides and reduce the insertion loss [41, 42]. Figure 4 (a) shows the change in the effective index of plasmonic and silicon waveguides by changing their width. Based on Figure 4 (a), for W_{Si} = 300 nm and W_{PL} = 130 nm, the two waveguides' effective index matched.

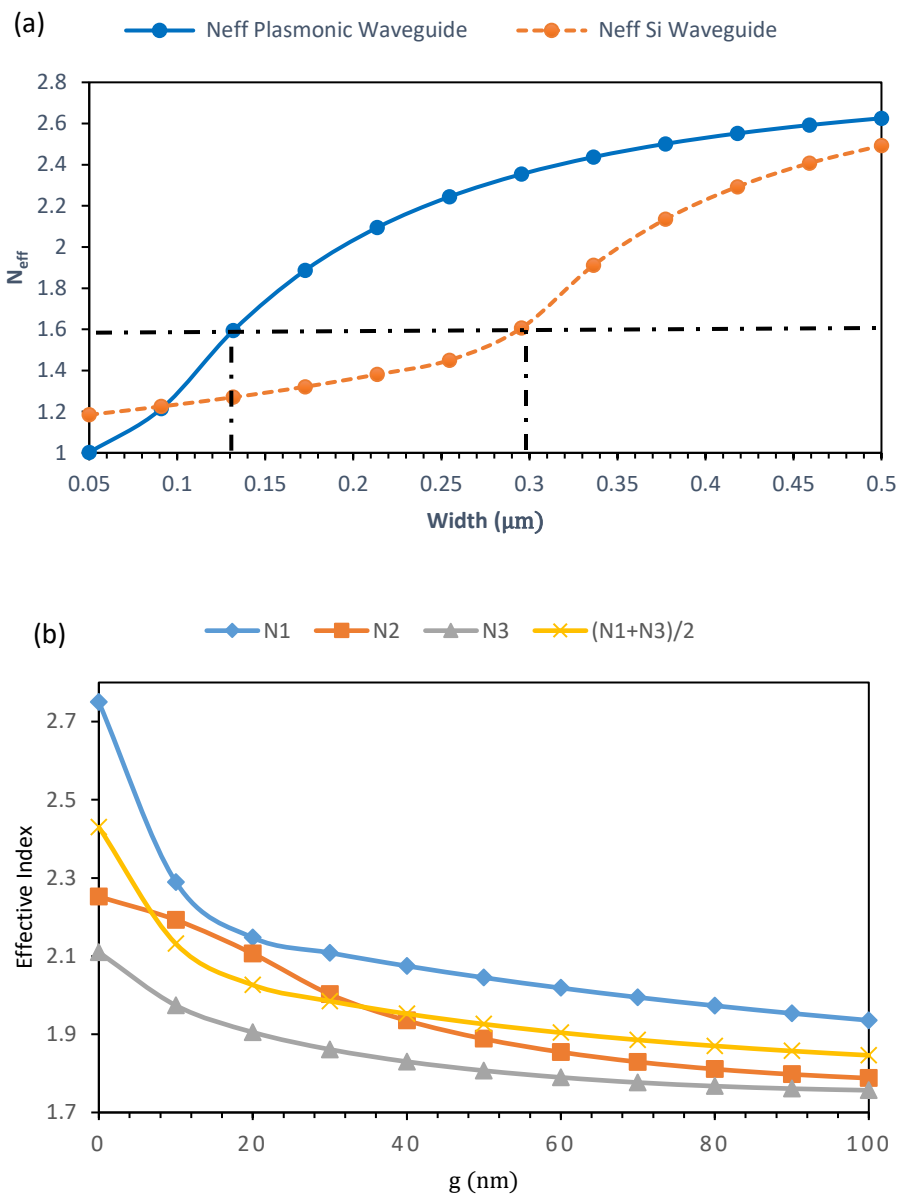

Figure 4: a) The effective index of the silicon waveguide and plasmonic waveguide (V=0 V) for the different values of wave guides width b) the effective index of eigenmode for different gap between the Si and plasmonic waveguides (H_{Si}=250nm, H_{PL}=566 nm, H_{ITO}=10nm, H_{HfO2}=10nm).

The coupling length (L_c) is calculated by coupling theory[34, 43, 44]. The device propagation mode has been found with cross-section simulation. n_1, n_2, and n_3 are the effective index of the eigenmodes, which are symmetric mode (mode 1), asymmetric mode (mode 2), and symmetric mode (mode 3), respectively. Eigenmodes modes should apply to equation 6 to achieve maximum output power in V=0 [34, 35, 44]:

$$2n_2 - n_1 - n_3 = 0 \rightarrow n_2 = \frac{n_1+n_3}{2} \qquad (6)$$

The effective index of eigenmode modes for different values of the gap (distance between the waveguides) is shown in figure 4 (b). g = 30nm has been considered based on figure 4 (b) and equation 6.

The coupling length is obtained by the following equation [34, 35, 44]:

$$L_c = \frac{\lambda}{2(n_1 - n_2)} \qquad (7)$$

L_c is equal to $L_c = 4.9\ \mu m$ (in the λ = 1.55μm). Figure 5 shows the coupling length with voltage change. By changing the voltage, the coupling length shows the dynamic behavior that results from the change of the real and imaginary parts of the effective index. Changing the coupling length disrupts the power coupling and thus has a role in attenuating the output power.

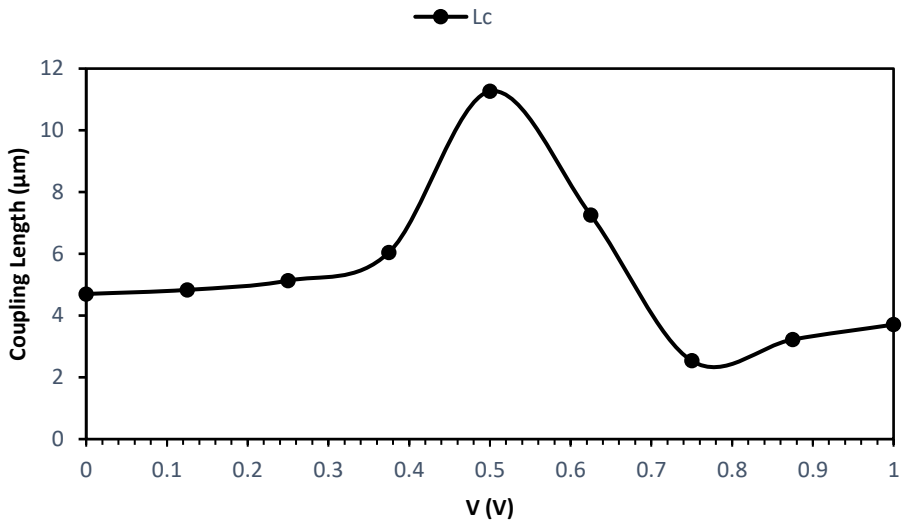

Figure 5: The coupling length with voltage change

4. Properties of the hybrid plasmonic modulator

The device performance's main characteristics are presented in this section. Modulation speed, power consumption, propagation loss, and extinction ratio (ER) are investigated. The on/off extinction ratio is about 14 dB/μm; ER equals the difference between the propagation loss at the zero voltage and 0.62 V (ER=Loss0.62V-Loss0V) [31]. Loss in zero voltage is 1.6 dB/μm; also, we set the device length equal to coupling length. Figure 6 shows the ER and propagation losses for different wavelengths. The proposed modulator's ER is better than modulators in [31, 45].

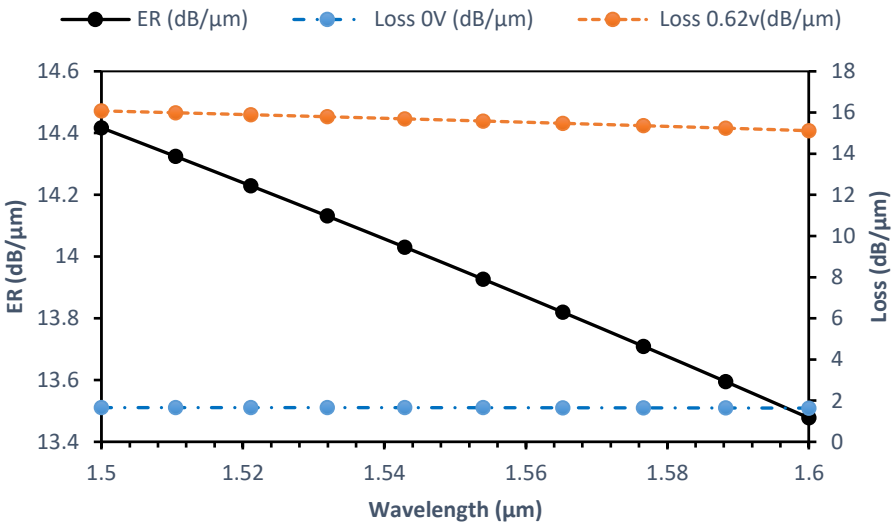

Figure 6: ER as a function of wavelength

The resistance and capacitance of the device limit the modulation speed of the optical modulator. Power consumption is also related to modulation voltage and capacitance.

Capacitance is calculated by equation 8. The capacitors are modeled with a parallel plate structure (graphene/ HfO_2/ITO interface) [31, 44]. With this definition, there are two capacitors in the structure.

$$C = \left(\varepsilon_0 \varepsilon_{ox} \frac{A}{W_{ox}}\right) = (W_{PL} \times L_c \times \varepsilon_0 \times \varepsilon_{HfO_2})/H_{HfO_2} \quad (8)$$

C_T=C+C= 28.2 fF. The modulation speed is equal to:

$$f = \frac{1}{2\pi RC} \quad (9)$$

R=500Ω is an internal impedance [46], 11.3 GHz is the modulation speed. Power consumption is equal to: $E_{bit} = CV_{on}^2/2 + CV_{off}^2/2$ and it is 5.4 fJ/bit [47].

The ER and power consumption of the proposed modulator are better than [12, 48-51], and modulation speed has improved compared to [48, 49]. The proposed modulator characteristics such as ER, f (3dB), Ebit are compared with similar structures in Table 1.

Table 1: Comparison of the proposed modulator with similar modulators

Device Type		IL (dB/µm)	ER (dB/µm)	E (fJ)	Modulation speed(GHz)	Device Length (µm)
ITO based Vertical structure[12]		0.03	4.8	14.8	363	5.53
Au VO_2 hybrid plasmonic[48]			8.9	a	>1	0.56
TiN/Cu/ITO structure[49]		0.88	3.95	400	11	1
Hybrid Si/VO_2[50]		0.1	4.4	a	a	1
plasmonic electro-absorption[51]	ITO based	0.025	3.07	178	8.84	0.5
	VO_2 based	0.651	5.85	400	52.6	0.5

This work	1.6	14	5.4	11.3	4.9

a:Not reported

5. Conclusion

The optical modulator based on coupling between waveguides with vertical plasmonic structure was proposed and designed. The graphene and ITO were used in the plasmonic region of the modulator to decrease the operating voltage and increase the light-matter interaction. The modulator had a high ER (14 dB/μm), a compact size (4.9 μm), and low power consumption of (5.4 fJ). The modulator also had a broadband performance. The modulator characteristic in comparison to other similar modulators showed significant improvement. This plasmonic modulator with high ER, relatively low IL, and broadband could be used compact size, energy-efficient and potentially fast on-chip communication interconnects for the photonic integrated circuit.

Funding

No funding

Conflicts of interest/Competing interests

'Not applicable'

Availability of data and material

'Not applicable'

Code availability

'Not applicable'

Authors' contributions

The authors' contributions are equal.

Ethics approval

Consent to participate

Consent for publication

References:

[1] Q. Xu, B. Schmidt, S. Pradhan, and M. Lipson, "Micrometre-scale silicon electro-optic modulator," *Nature,* vol. 435, no. 7040, pp. 325-7, May 19 2005.10.1038/nature03569

[2] K. Preston, S. Manipatruni, A. Gondarenko, C. B. Poitras, and M. Lipson, "Deposited silicon high-speed integrated electro-optic modulator," *Opt Express,* vol. 17, no. 7, pp. 5118-24, Mar 30 2009.10.1364/oe.17.005118

[3] Z. Li, L. Bai, X. Li, E. Gu, L. Niu, and X. Zhang, "U-shaped micro-ring graphene electro-optic modulator," *Optics Communications,* vol. 428, pp. 200-205, 2018.

[4] F. Qiu and Y. Han, "Electro-optic polymer ring resonator modulators," *Chinese Optics Letters,* vol. 19, no. 4, p. 041301, 2021.
[5] M. Mahmoud, C. Bottenfield, L. Cai, and G. Piazza, "Fully integrated lithium niobate electro-optic modulator based on asymmetric Mach-Zehnder interferometer etched in LNOI platform," in *2017 IEEE Photonics Conference (IPC)*, 2017, pp. 223-224: IEEE.
[6] L. Jiang, X. Chen, K. Kim, G. de Valicourt, Z. R. Huang, and P. Dong, "Electro-optic crosstalk in parallel silicon photonic Mach-Zehnder modulators," *Journal of Lightwave Technology,* vol. 36, no. 9, pp. 1713-1720, 2018.
[7] V. E. Babicheva *et al.*, "Towards CMOS-compatible nanophotonics: Ultra-compact modulators using alternative plasmonic materials," *Optics express,* vol. 21, no. 22, pp. 27326-27337, 2013.
[8] B. H. Siahkal-Mahalle and K. Abedi, " The Effect of Carrier Distribution on Performance of ENZ-Based Electro-Absorption Modulator," *Plasmonics,* vol. 15, no. 7, p. 1689-1697, 2020.
[9] W. Du *et al.*, "Electrically controllable directional coupler based on tunable hybrid graphene nanoplasmonic waveguide," *Optics Communications,* vol. 430, pp. 450-455, 2019.
[10] M. Liu *et al.*, "A graphene-based broadband optical modulator," *Nature,* vol. 474, no. 7349, pp. 64-7, Jun 2 2011.10.1038/nature10067
[11] H. M. Wong and A. S. Helmy, "Performance enhancement of nanoscale VO 2 modulators using hybrid plasmonics," *Journal of Lightwave Technology,* vol. 36, no. 3, pp. 797-808, 2017.
[12] C. Lin and A. S. Helmy, "Dynamically reconfigurable nanoscale modulators utilizing coupled hybrid plasmonics," *Sci Rep,* vol. 5, no. 1, p. 12313, Jul 20 2015.10.1038/srep12313
[13] U. Koch, C. Hössbacher, J. Niegemann, C. Hafner, and J. Leuthold, "Digital plasmonic absorption modulator exploiting epsilon-near-zero in transparent conducting oxides," *IEEE Photonics Journal,* vol. 8, no. 1, pp. 1-13, 2016.
[14] M. K. Shah, R. Lu, and Y. Liu, "Enhanced performance of ITO-assisted electro-absorption optical modulator using sidewall angled silicon waveguide," *IEEE Transactions on Nanotechnology,* vol. 17, no. 3, pp. 412-418, 2018.
[15] L. Jin, Q. Chen, W. Liu, and S. Song, "Electro-absorption modulator with dual carrier accumulation layers based on epsilon-near-zero ITO," *Plasmonics,* vol. 11, no. 4, pp. 1087-1092, 2016.
[16] M. G. Wood *et al.*, "Gigahertz speed operation of epsilon-near-zero silicon photonic modulators," *Optica,* vol. 5, no. 3, pp. 233-236, 2018.
[17] J. T. Kim, "CMOS-compatible hybrid plasmonic modulator based on vanadium dioxide insulator-metal phase transition," *Opt Lett,* vol. 39, no. 13, pp. 3997-4000, Jul 1 2014.10.1364/OL.39.003997
[18] S. Campione *et al.*, "Submicrometer epsilon-near-zero electroabsorption modulators enabled by high-mobility cadmium oxide," *IEEE Photonics Journal,* vol. 9, no. 4, pp. 1-7, 2017.
[19] B. H. Huang, W. B. Lu, X. B. Li, J. Wang, and Z. G. Liu, "Waveguide-coupled hybrid plasmonic modulator based on graphene," *Appl Opt,* vol. 55, no. 21, pp. 5598-602, Jul 20 2016.10.1364/AO.55.005598
[20] J. Zhu, J. Cheng, L. Zhang, and Q. H. Liu, "Modeling of 2D graphene material for plasmonic hybrid waveguide with enhanced near-infrared modulation," *Materials Letters,* vol. 186, pp. 53-56, 2017.
[21] H. W. Lee *et al.*, "Nanoscale conducting oxide PlasMOStor," *Nano Lett,* vol. 14, no. 11, pp. 6463-8, Nov 12 2014.10.1021/nl502998z
[22] Z. Wu and Y. Xu, "Design of a graphene-based dual-slot hybrid plasmonic electro-absorption modulator with high-modulation efficiency and broad optical bandwidth for on-chip communication," *Appl Opt,* vol. 57, no. 12, pp. 3260-3267, Apr 20 2018.10.1364/AO.57.003260
[23] X. Chen *et al.*, "A broadband optical modulator based on a graphene hybrid plasmonic waveguide," *Journal of Lightwave Technology,* vol. 34, no. 21, pp. 4948-4953, 2016.
[24] M. Liu *et al.*, "A graphene-based broadband optical modulator," *Nature,* vol. 474, no. 7349, pp. 64-67, 2011.
[25] B. Sensale-Rodriguez *et al.*, "Extraordinary control of terahertz beam reflectance in graphene electro-absorption modulators," *Nano Lett,* vol. 12, no. 9, pp. 4518-22, Sep 12 2012.10.1021/nl3016329

[26] D. Ansell, I. P. Radko, Z. Han, F. J. Rodriguez, S. I. Bozhevolnyi, and A. N. Grigorenko, "Hybrid graphene plasmonic waveguide modulators," *Nat Commun,* vol. 6, no. 1, p. 8846, Nov 10 2015.10.1038/ncomms9846

[27] S. Han, S. Kim, S. Kim, T. Low, V. W. Brar, and M. S. Jang, "Complete Complex Amplitude Modulation with Electronically Tunable Graphene Plasmonic Metamolecules," *ACS Nano,* vol. 14, no. 1, pp. 1166-1175, Jan 28 2020.10.1021/acsnano.9b09277

[28] F. Sun *et al.*, "An all-optical modulator based on a graphene–plasmonic slot waveguide at 1550 nm," *Applied Physics Express,* vol. 12, no. 4, p. 042009, 2019.

[29] C. Ye, S. Khan, Z. R. Li, E. Simsek, and V. J. Sorger, "λ-size ITO and graphene-based electro-optic modulators on SOI," *IEEE Journal of Selected Topics in Quantum Electronics,* vol. 20, no. 4, pp. 40-49, 2014.

[30] S. Das, A. Salandrino, J. Z. Wu, and R. Hui, "Near-infrared electro-optic modulator based on plasmonic graphene," *Opt Lett,* vol. 40, no. 7, pp. 1516-9, Apr 1 2015.10.1364/OL.40.001516

[31] J.-S. Shin and J. T. Kim, "Broadband silicon optical modulator using a graphene-integrated hybrid plasmonic waveguide," *Nanotechnology,* vol. 26, no. 36, p. 365201, 2015.

[32] L. Akbari and K. Abedi, " A highly sensitive and tunable plasmonic sensor based on a graphene tubular resonator," *Optics Communications, vol. 458, pp. 124686, 2020.*

[33] E. Feigenbaum, K. Diest, and H. A. Atwater, "Unity-order index change in transparent conducting oxides at visible frequencies," *Nano letters,* vol. 10, no. 6, pp. 2111-2116, 2010.

[34] J. Chee, S. Zhu, and G. Lo, "CMOS compatible polarization splitter using hybrid plasmonic waveguide," *Optics Express,* vol. 20, no. 23, pp. 25345-25355, 2012.

[35] F. Lou, D. Dai, and L. Wosinski, "Ultracompact polarization beam splitter based on a dielectric–hybrid plasmonic–dielectric coupler," *Optics letters,* vol. 37, no. 16, pp. 3372-3374, 2012.

[36] A. V. Krasavin and A. V. Zayats, "Photonic signal processing on electronic scales: electro-optical field-effect nanoplasmonic modulator," *Phys Rev Lett,* vol. 109, no. 5, p. 053901, Aug 3 2012.10.1103/PhysRevLett.109.053901

[37] W. Jiang, J. Miao, and T. Li, "Silicon Mode-Selective Switch via Horizontal Metal-Oxide-Semiconductor Capacitor Incorporated With ENZ-ITO," *Scientific reports,* vol. 9, no. 1, pp. 1-12, 2019.

[38] A. Alù, M. G. Silveirinha, and N. Engheta, "Transmission-line analysis of ε-near-zero–filled narrow channels," *Physical Review E,* vol. 78, no. 1, p. 016604, 2008.

[39] A. Eslami, M. Sadeghi, and Z. Adelpour, "Plasmonic modulator utilizing graphene-HfO2-ITO stack embedded in the silicon waveguide," *Optik,* vol. 227, p. 165608, 2021.

[40] C. Lin and A. S. Helmy, "Dynamically reconfigurable nanoscale modulators utilizing coupled hybrid plasmonics," *Scientific reports,* vol. 5, p. 12313, 2015.

[41] W. P. Huang and J. Mu, "Complex coupled-mode theory for optical waveguides," *Opt Express,* vol. 17, no. 21, pp. 19134-52, Oct 12 2009.10.1364/OE.17.019134

[42] M. Y. Abdelatty, M. M. Badr, and M. A. Swillam, "Compact silicon electro-optical modulator using hybrid ITO tri-coupled waveguides," *Journal of Lightwave Technology,* vol. 36, no. 18, pp. 4198-4204, 2018.

[43] W. Jiang, J. Miao, and T. Li, "Silicon Mode-Selective Switch via Horizontal Metal-Oxide-Semiconductor Capacitor Incorporated With ENZ-ITO," *Sci Rep,* vol. 9, no. 1, p. 17777, Nov 28 2019.10.1038/s41598-019-54332-6

[44] C. Ye, K. Liu, R. A. Soref, and V. J. Sorger, "A compact plasmonic MOS-based 2× 2 electro-optic switch," *Nanophotonics,* vol. 4, no. 3, pp. 261-268, 2015.

[45] C. Lin and A. S. Helmy, "Dynamically reconfigurable nanoscale modulators utilizing coupled hybrid plasmonics," *Scientific reports,* vol. 5, no. 1, pp. 1-10, 2015.

[46] K. J. Ooi *et al.*, "Dirac terahertz plasmonics in two and three dimensions," *Optics Communications,* vol. 462, p. 125319, 2020.

[47] A. Shetty *et al.*, "Temperature dependent electrical characterisation of Pt/HfO2/n-GaN metal-insulator-semiconductor (MIS) Schottky diodes," *AIP Advances,* vol. 5, no. 9, p. 097103, 2015.

[48] P. Markov, K. Appavoo, R. F. Haglund, Jr., and S. M. Weiss, "Hybrid Si-VO(2)-Au optical modulator based on near-field plasmonic coupling," *Opt Express,* vol. 23, no. 5, pp. 6878-87, Mar 9 2015.10.1364/OE.23.006878

[49] S. Zhu, G. Q. Lo, and D. L. Kwong, "Design of an ultra-compact electro-absorption modulator comprised of a deposited TiN/HfO(2)/ITO/Cu stack for CMOS backend integration," *Opt Express,* vol. 22, no. 15, pp. 17930-47, Jul 28 2014.10.1364/OE.22.017930

[50] M. Sadeghi, B. Janjan, M. Heidari, and D. Abbott, "Mid-infrared hybrid Si/VO 2 modulator electrically driven by graphene electrodes," *Optics express,* vol. 28, no. 7, pp. 9198-9207, 2020.

[51] H. R. Das and S. C. Arya, "Performance improvement of VO2 and ITO based plasmonic electro-absorption modulators at 1550 nm application wavelength," *Optics Communications,* vol. 479, p. 126455, 2021.

Figures

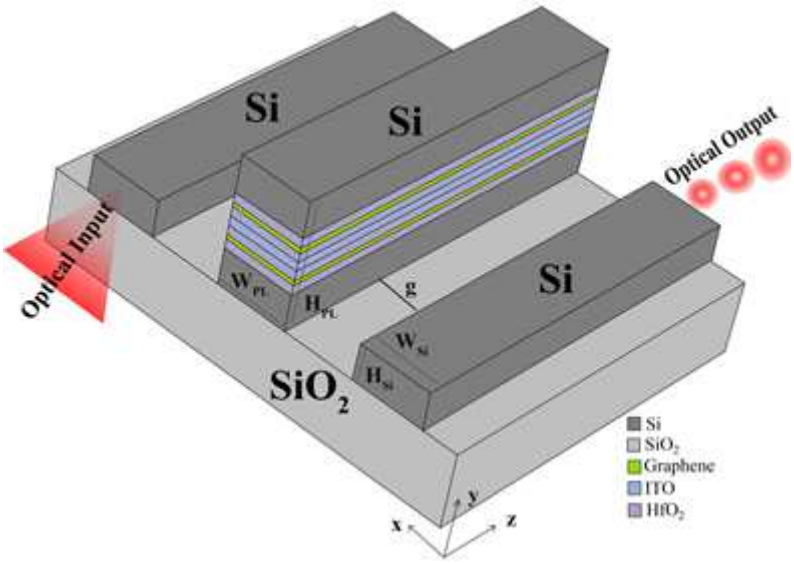

Figure 1

3D view of the proposed structure

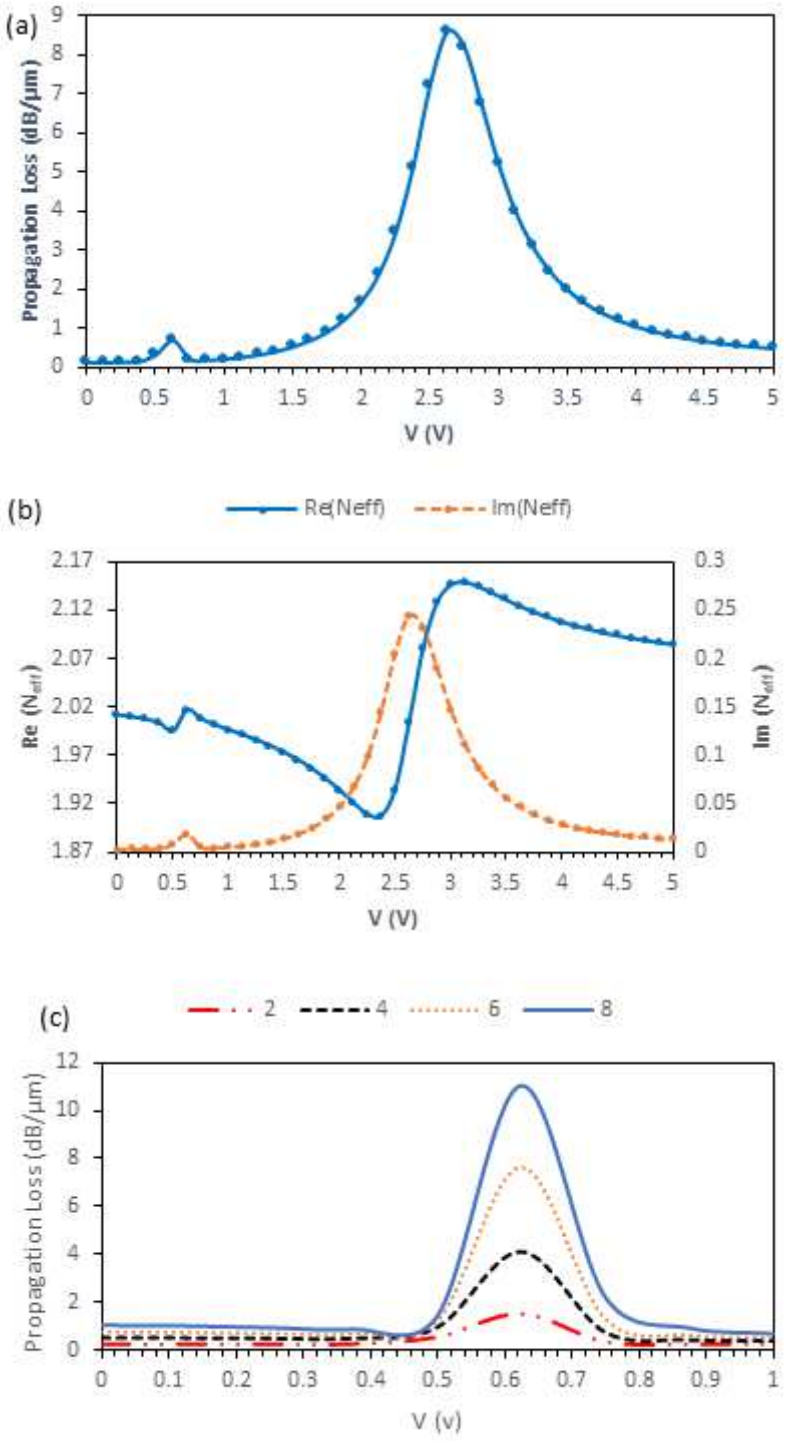

Figure 2

a) propagation loss for different voltage values (monolayer graphene) b) The real and imaginary part of the refractive index (graphene monolayer) c) propagation loss for different voltage values (multilayer graphene: 2,4,6,8 layer) (WPL=130nm, HITO=10nm, HHfO2=10nm)

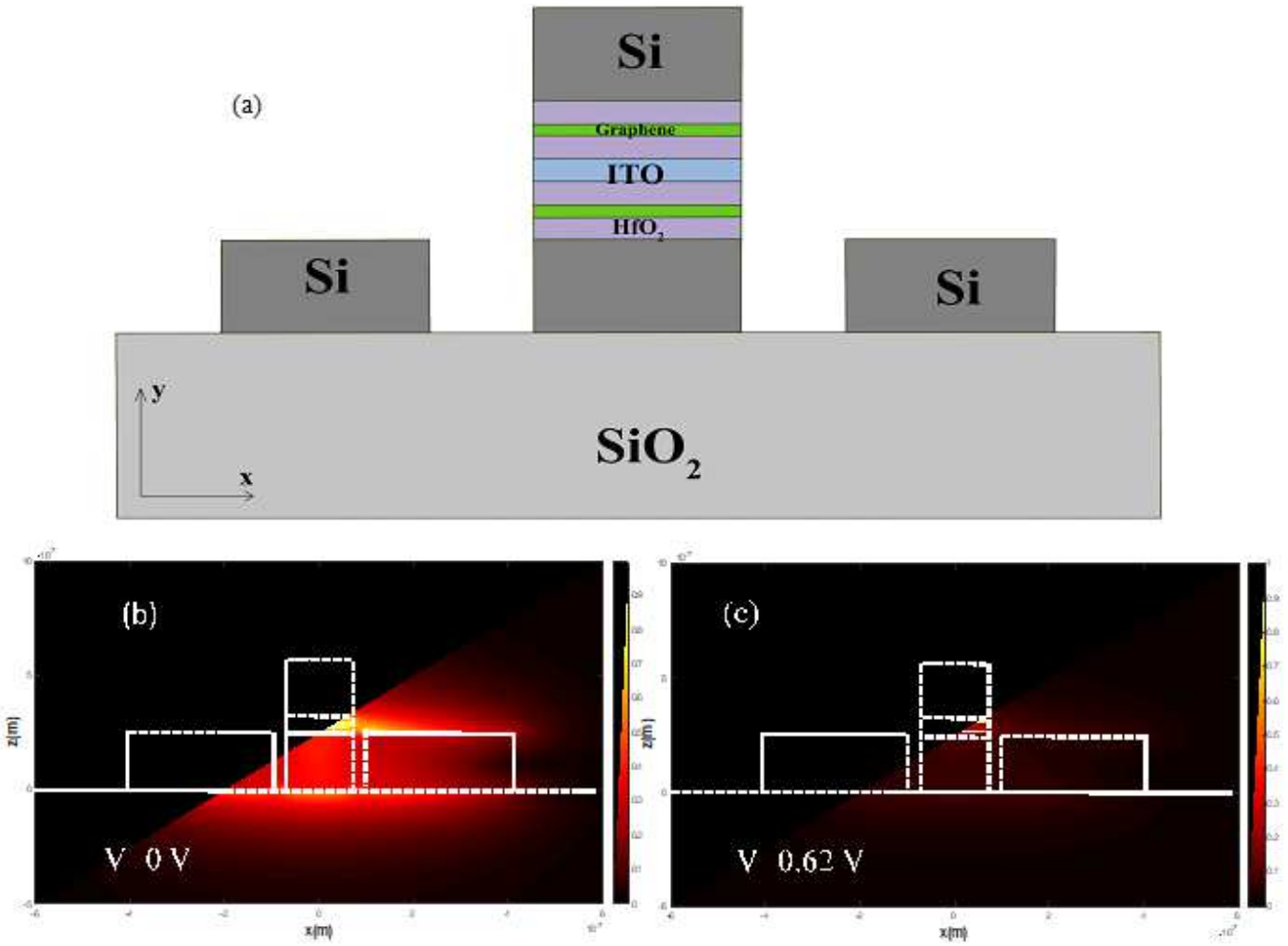

Figure 3

a) Proposed modulators cross-section view, the intensity of the guided mode of the electric field in b) On state (V=0) c) Off state (V=0.62V) (WSi=300nm, HSi=250nm, HPL=566 nm ,WPL=130nm, HITO=10nm, HHfO2=10nm, g=30 nm)

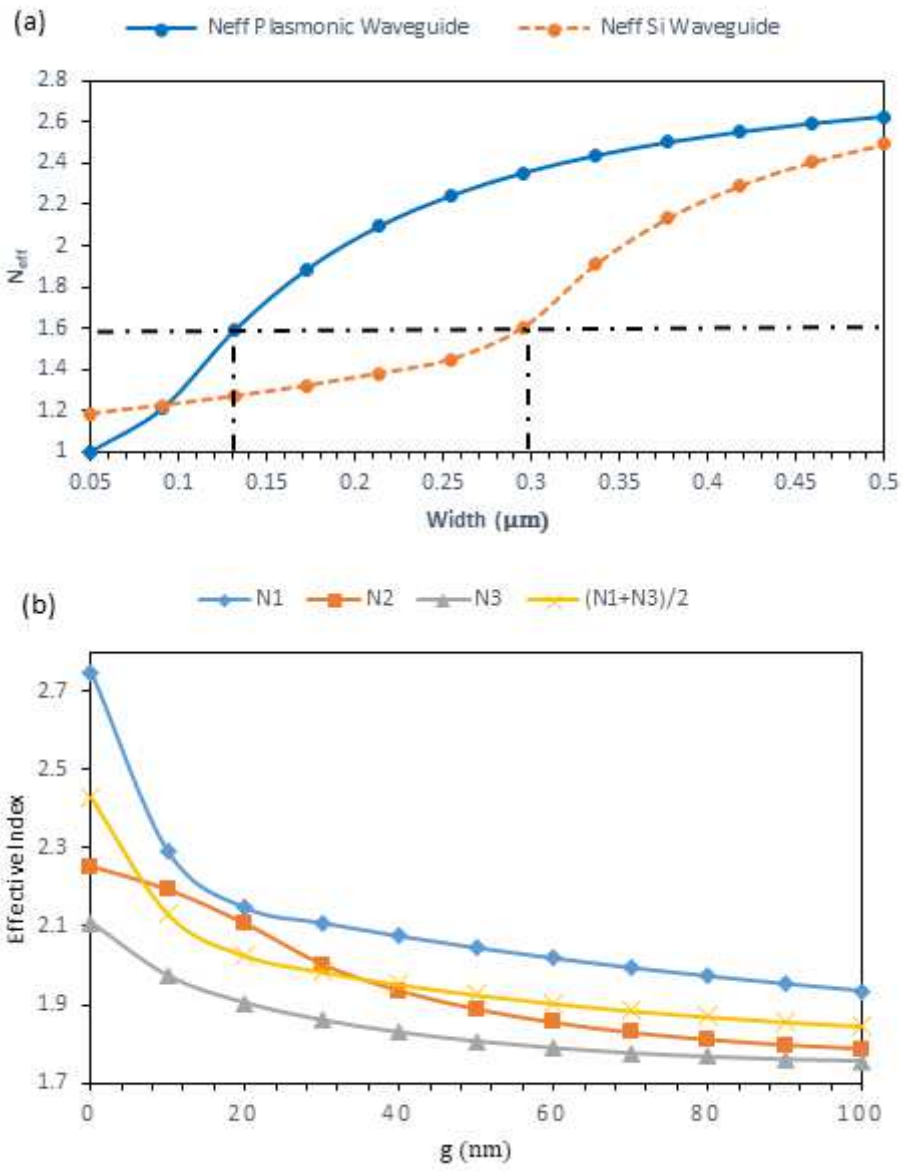

Figure 4

a) The effective index of the silicon waveguide and plasmonic waveguide (V=0 V) for the different values of wave guides width b) the effective index of eigenmode for different gap between the Si and plasmonic waveguides (HSi=250nm, HPL=566 nm, HITO=10nm, HHfO2=10nm).

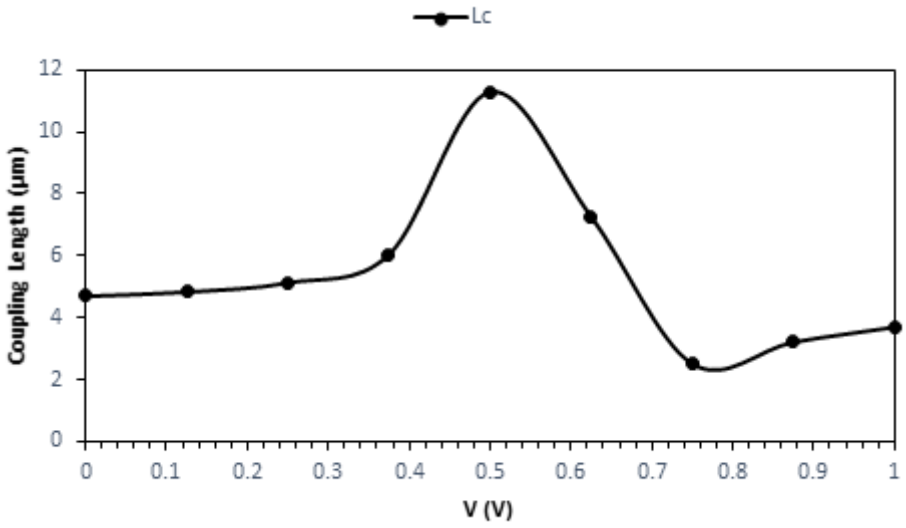

Figure 5

The coupling length with voltage change

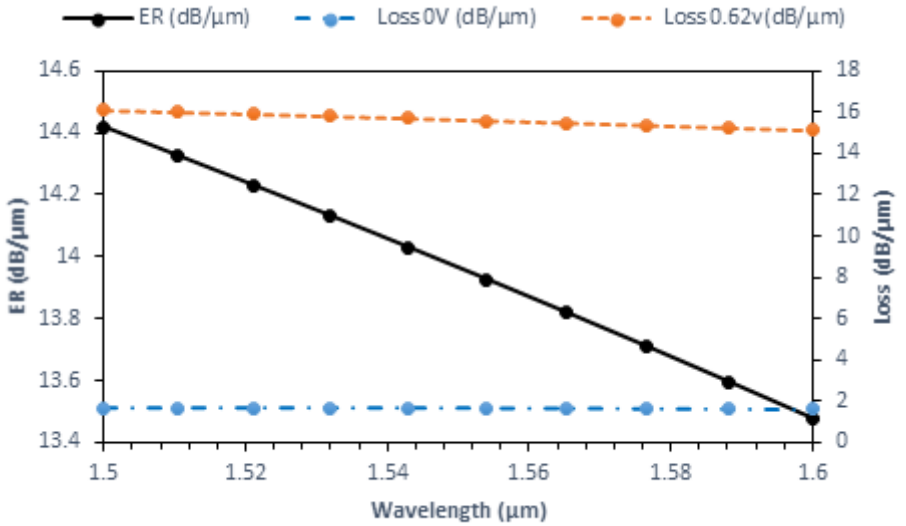

Figure 6

ER as a function of wavelength